metals

MDPI

Review

A Review of Molecular Dynamics Simulation of Different Ti-Al-Based Alloys

Ningning Li [1,2], Zhenjie Hao [1,2], Lei Xu [1,2,*], Mingqi Tang [1,2], Leyu Wei [1,2] and Lifei Wang [3,*]

[1] School of Materials Science and Engineering, North China University of Water Resources and Electric Power, Zhengzhou 450045, China; liningning@ncwu.edu.cn (N.L.); haozhenjie2000@163.com (Z.H.); tangmingqi@ncwu.edu.cn (M.T.); weileiyu@ncwu.edu.cn (L.W.)
[2] Henan Engineering Research Center on Special Materials and Applications of Water Conservancy and Hydropower Engineering, Zhengzhou 450045, China
[3] College of Materials Science and Engineering, Taiyuan University of Technology, Taiyuan 030024, China
* Correspondence: xulei2022@ncwu.edu.cn (L.X.); wanglifei@tyut.edu.cn (L.W.)

Abstract: Ti-Al-based alloys, particularly two-phase TiAl and Ti_3Al alloys, have garnered significant attention as potential replacements for various high-temperature structural materials due to their exceptional properties, including low density, oxidation resistance, and high strength at elevated temperatures. Despite these advantages, experimental studies on the microstructure evolution of Ti-Al-based alloys under complex conditions remain challenging to observe and characterize. This review article examines the current research on molecular dynamics (MD) simulations of Ti-Al-based alloys, focusing on two-phase Ti-Al alloys, Ti-Al amorphous alloys, Ti-Al composite materials, and the welding and multi-layer/film applications of Ti-Al alloys. This review highlights the unique capabilities of MD simulations in predicting the behavior of Ti-Al-based alloys and addresses existing scientific challenges. Furthermore, this article discusses future research directions and development prospects in this field.

Keywords: Ti-Al-based alloys; structural materials; molecular dynamics; material data

Citation: Li, N.; Hao, Z.; Xu, L.; Tang, M.; Wei, L.; Wang, L. A Review of Molecular Dynamics Simulation of Different Ti-Al-Based Alloys. *Metals* **2024**, *14*, 1018. https://doi.org/10.3390/met14091018

Academic Editor: Alain Pasturel

Received: 18 August 2024
Revised: 3 September 2024
Accepted: 4 September 2024
Published: 6 September 2024

1. Introduction

The rapid advancements in the aerospace and automotive industries have led to an increased demand for metal structural materials, particularly those used in engines and thermal protection systems [1–3]. Enhancing the operating temperature and reducing the weight of engine components are two critical strategies for improving the performance of existing engines and developing new engines with high thrust-to-weight ratios. Consequently, the search for new lightweight, high-temperature structural materials to enhance efficiency and conserve energy has become a key research focus. Numerous countries have shown significant interest in titanium and aluminum compounds, conducting extensive and in-depth research. Especially Ti_3Al- and TiAl-based superalloys, achieving remarkable results [4–6].

Ti-Al-based alloys have emerged as promising candidates to replace Ni-based high-temperature alloys. This is primarily due to their low density, high strength retention at elevated temperatures, excellent creep resistance, and high specific strength [7–9]. Within the Ti-Al binary system, three intermetallic compounds—Ti_3Al, TiAl, and $TiAl_3$—have garnered extensive research and attention. Additionally, based on Ti_3Al research, the Ti_2AlNb titanium alloy has been developed [10–13]. A comparative performance analysis of Ti-, TiAl-, and Ti_3Al-based alloys is presented in Table 1.

TiAl is a typical berthollide compound with a broad compositional range, from 48% to 69.5% aluminum (atomic fraction), and remains stable below its melting point of 1460 °C. TiAl exhibits an $L1_0$-ordered superlattice structure, characterized by a square lattice with parameters a = 0.398 nm, c = 0.404 nm, and a c/a ratio of 1.015. This c/a

ratio varies from 1.01 to 1.03 as the aluminum content increases. The Ti_3Al intermetallic compound has a $D0_{19}$ structure, which is an ordered variant of the α-Ti structure, also known as the α_2 phase [14–16]. Studies on the resilience mechanism of Ti_3Al have revealed that increasing the Nb content (primarily Nb, with some Mo and V) leads to the formation of a new phase, Ti_2AlNb [17]. When the Nb content reaches 25%, a Ti_2AlNb combination is formed. Face-centered cubic (FCC) $TiAl_3$-type alloys, with their low density and high melting points, show significant promise as high-temperature-resistant metal composites [18]. The lattice parameters for the $TiAl_3$-$D0_{22}$ phase are reported as a = b = 0.3856 nm and c = 0.8622 nm, giving a c/a ratio of 2.236 [19].

Table 1. Performance comparison of Ti-, TiAl-, and Ti_3Al-based alloys.

Performance	Ti-Based Alloys	TiAl-Based Alloys	Ti_3Al-Based Alloys
Crystal structure	hcp/bcc	$L1_0$	$D0_{19}$
Density/g·cm^{-3}	4.5	4.1–4.7	3.7~4.3
Elastic modulus/GPa	96–115	100~145	160~180
Yield strength/MPa	380–1150	700~990	400~800
Tensile strength/MPa	480~1200	800~1140	450~1000

The properties of Ti-Al-based alloys are influenced by factors such as alloying elements, processing methods, and microstructure variations. However, experimental deformation tests are often tedious, costly, and challenging to observe directly at the atomic scale. Advances in computer technology have popularized molecular dynamics (MD) as an effective simulation method for material calculations [20–22]. MD studies, conducted using the LAMMPS package, utilize atomic interaction potentials to simulate material behavior. Among the various potentials available, such as MEAM and EAM, the EAM potential is particularly effective for MD characterization [23]. This is due to its ability to accurately model interactions between similar and dissimilar atoms, facilitating the examination of the effects of externally applied forces on all particles [24–26].

The MD simulation is a powerful method for uncovering the deformation mechanisms of metal materials at the atomic scale [27–29]. It allows the dynamic evolution processes observed under various loading conditions, such as the nucleation, propagation, and interaction of atomic structures. Additionally, MD simulations provide valuable insights into the effects of microstructure features and ambient temperature on mechanical properties and failure modes [30–32], making them essential for understanding the plastic deformation mechanisms of metal materials [33–35]. For instance, Medyanik et al. [36] demonstrated that the coherent interface in a Cu-Ni bilayered composite acts as a strong barrier to dislocation propagation during nanoindentation, significantly strengthening the composite. Similarly, Shimono et al. [37] conducted MD simulations to study the recrystallization process of Ti-Al alloys in an amorphous state, revealing that the alloy's ability to form an amorphous structure is influenced by its aluminum content.

Currently, MD simulations have been widely applied to the study of Ti-Al-based alloys. For instance, researchers have investigated the rapid cooling of Ti_3Al to form amorphous materials, determining the relationship between cooling rate and amorphous formation ability using the EAM potential [37–39]. Studies have also explored the thermophysical properties of molten titanium–aluminum, including density and specific heat [40]. Subsequent research has expanded into areas such as layered composites [41,42], welding [43,44], and the effects of additional alloying elements on titanium–aluminum alloys [45–47].

In this study, we review the MD simulations related to different Ti-Al-based alloys, aiming to present recent research progress. Section 2 discusses the simulation methods employed for different types of Ti-Al alloys and analyzes the resulting data. Finally, Section 3 addresses the development trends, challenges, and future directions for applying MD simulations to Ti-Al-based alloys.

2. Prediction of Different Ti-Al-Based Alloys

The thermophysical properties, particularly in the under-cooled regime, are crucial for understanding and defining the thermodynamic state of Ti-Al-based systems. Properties such as specific heat and density of liquid alloys in this regime are of significant interest [40]. MD simulations are highly effective in studying these properties, as well as the local structure and diffusion in liquid Ti_xAl_{1-x} alloys, using the EAM potential and NPT ensemble [48]. Additionally, MD simulations have been applied to investigate transitions from the β phase to the α phase, elastic constants, structural and deformation behaviors, and the micro-mechanisms of cold deformation in Ti-Al alloys [49–51].

MD simulations are being increasingly used to explore the dynamic properties of Ti-Al-based alloys, offering high efficiency in simulating atomic-level processes over extensive spatial and temporal scales [52–56]. MD simulations can be used for calculations involving various ensembles, such as NPT, NVE, and NVT. This method, grounded in Newtonian determinism, provides higher accuracy and effectiveness in macroscopic property calculations compared to Monte Carlo methods and is widely applicable across fields like physics, chemistry, biology, materials science, medicine, etc. [57]. In this section, we briefly introduce the application of MD simulations in studying two-phase alloys, amorphous alloys, composite materials, welding, and multi-layer/film materials in Ti-Al alloys, as illustrated in Figure 1.

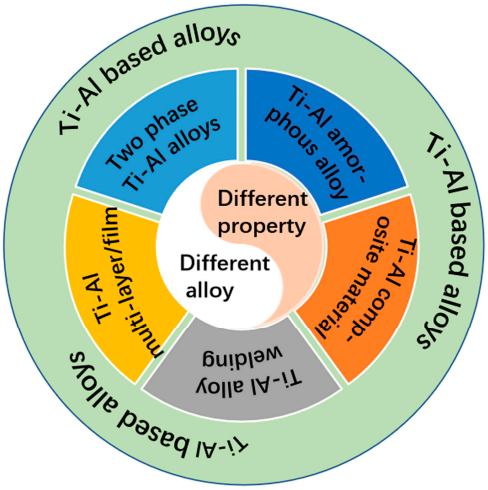

Figure 1. Application of molecular dynamics simulation on different types of Ti-Al-based alloys.

2.1. Simulation of Two-Phase Ti-Al Alloys

Ti-Al alloys have been extensively studied to address challenges related to ductility and damage tolerance. Research has focused on single-phase γ-TiAl [58], Ti_3Al alloys [59], polysynthetically twinned crystals (PTCs) [56], deformation twinning [60], and various compositions of Ti-Al alloys [61,62]. Key areas of investigation include the effects of residual stress, deformation, and crystal structure [49,63,64].

Hariprasath Ganesan [64] studied the high-temperature separation behavior of lamellar interfaces in γ-TiAl under tensile loading, with the main results shown in Figure 2. This study employed two different atomistic interface models: a defect-free model (Type 1) and a model with preexisting voids (Type 2), as illustrated in Figure 2a. In Figure 2b, the first row presents the constructed atomistic models of the four interlamellar interfaces in TiAl after initial energy minimization. The second row displays the centrosymmetry parameter (CSP) for each atom in this initial configuration, which measures local lattice disorders caused by defects, surfaces, or interfaces. Figure 2c shows the global normal stress for Type-1 models of the four single interlamellar interfaces within the simulation box. A consistent relationship between stress and strain is observed for all temperatures, interfaces, and strain rates up to the yield stress, characterized by significant dislocation nucleation.

Figure 2d presents the global stress–strain curves for the Type-2 interface models, which contain a preexisting void. The presence of the void-type defect reduces the interface strength due to high local stress concentrations around the void, leading to lower global loads for interatomic bond breakage. Consequently, compared to the Type-1 models, the yield stress is reduced for all interfaces, with the high-stress regions near the void becoming dominant dislocation sources [64].

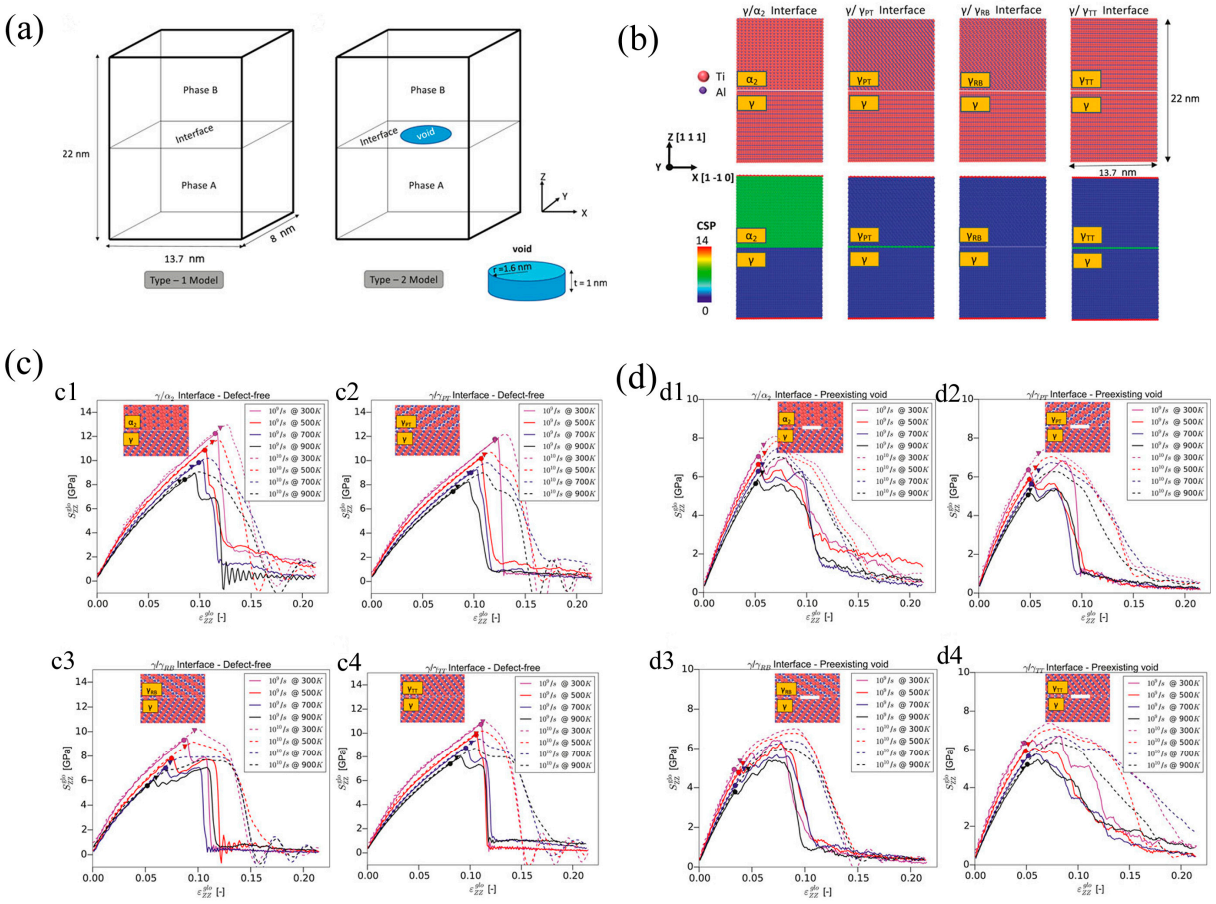

Figure 2. Partial study on high-temperature separation behavior of layered interface under tensile load of γ-TiAl. γ: TiAl, α_2: Ti_3Al, a pseudo twin (PT), rotational boundary (RB), and true twin (TT) configuration, denoted as γ/γ_{PT}, γ/γ_{RB}, and γ/γ_{TT} interfaces. (**a**) The two types of single interface models used herein. (**b**) First row: simulation system for the defect-free interfaces; second row: computed centrosymmetry parameter (CSP) to categorize the bulk constituent phase and interface. (**c**) Stress–strain curves under normal loading for Type-1 model interfaces, (**c1**) γ/α_2, (**c2**) γ/γ_{PT}, (**c3**) γ/γ_{PB}, and (**c4**) γ/γ_{TT}. (**d**) Stress–strain curves under normal loading for Type-2 model (with preexisting void) interfaces, (**d1**) γ/α_2, (**d2**) γ/γ_{PT}, (**d3**) γ/γ_{PB}, and (**d4**) γ/γ_{TT}. (Reprinted with permission from ref. [64]. Copyright 2021, Frontiers in Materials).

Roman E. Voskoboinikov [65] utilized MD simulations to study the radiation damage in the $D0_{19}$ Ti_3Al intermetallic compound. His findings revealed that Ti_3Al exhibited excellent resistance to the formation of primary radiation defects across the entire range of simulated temperatures and PKA energies. The number of Frenkel pairs generated in collision cascades in Ti_3Al is significantly lower than in α-Zr under identical irradiation conditions, particularly at high PKA energies and temperatures. This phenomenon suggests that Ti_3Al-based intermetallic alloys could benefit from enhanced oxidation and corrosion resistance through ion beam treatment followed by post-irradiation annealing.

2.2. Simulation of Ti-Al Amorphous Alloys

The microstructure of Ti-Al alloys can be controlled through amorphous metastable states, making it essential to understand the micro-mechanisms of amorphous phase formation and crystallization. The excessive vibration observed in metallic glasses, known as boson peaks, is a common characteristic of amorphous phases [66]. MD simulations have shown that these vibrational modes are closely related to local atomic structures and coordinated nanoscale motions. Research in this area includes the formation of amorphous Ti_3Al through rapid cooling [39], the thermal expansion and recrystallization of amorphous Al and Ti [67], the formation of amorphous structures by encapsulating Ti and Al nanoparticles [68,69], and the local atomic structural order in $TiAl_3$ metallic glass [70].

Xie et al. [71] investigated the glass formation and icosahedral intermediate-range order in liquid titanium–aluminum alloys. The results indicate that the icosahedron is an appropriate structural unit to describe the glass formation process of liquid and amorphous Ti-Al alloys. Additionally, hexagonally connected icosahedral clusters, linked by volume sharing, exhibit good structural stability and continuity, acting as tightly connected junctions. These clusters extend into nearby regions, enhancing structural integrity. The rapid solidification process and the formation of hexagonal structures effectively reflect the glass-forming ability of different Ti-Al alloy compositions. Part of the research findings are illustrated in Figure 3. Figure 3a shows the evolution of the simulation box with a structural type of Ti_3Al alloy during rapid solidification. Figure 3b presents sectional drawings of the center atoms of icosahedral clusters in $TiAl_3$ and TiAl alloys during rapid solidification. Figure 3c,d demonstrate that the fuller growth of IMRO structures in Ti-Al alloys results in the formation of more hexagonally connected icosahedral clusters after rapid quenching. The evolution of hexagonal structures in $TiAl_3$ alloys indicates the excellent structural stability and continuity of hexagonally connected icosahedral clusters during rapid solidification.

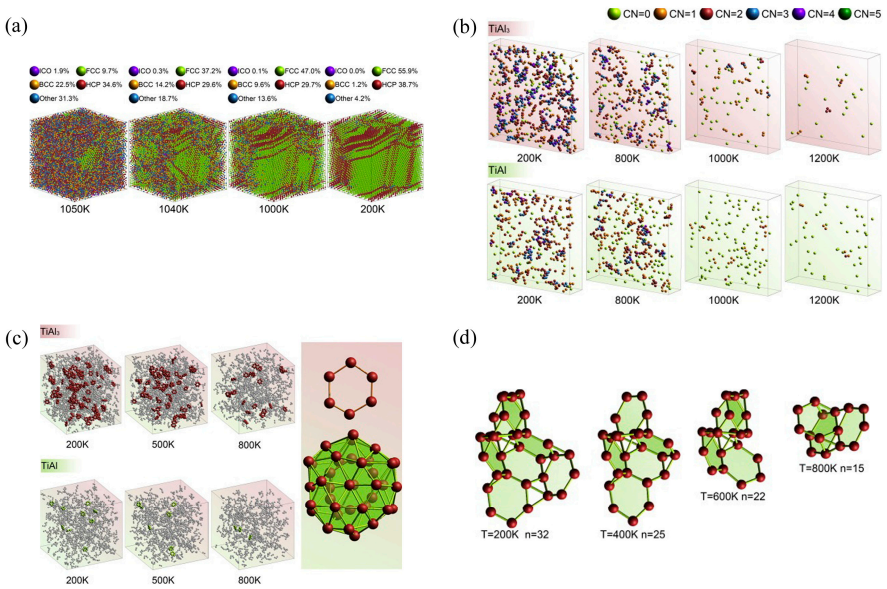

Figure 3. Glass formation and icosahedral medium-range order in liquid Ti-Al alloys. (**a**) Evolution of the simulation box with a structural type of Ti_3Al alloy during rapid solidification. (**b**) Sectional drawings of center atoms of icosahedral clusters in $TiAl_3$ and TiAl alloys during rapid solidifications. (**c**) Evolutions of center atoms of hexagonally connected icosahedral clusters in $TiAl_3$ and TiAl alloys during rapid solidifications. The red and green balls represent center atoms of hexagonally connected icosahedral clusters in $TiAl_3$ and TiAl alloys, respectively. The inset shows the formation of hexagonally connected icosahedral clusters. (For interpretation of the references to color in this figure legend, the reader is referred to the web version of this article). (**d**) Growth of center atoms of the hexagonally connected icosahedral clusters in a $TiAl_3$ alloy during rapid solidification. (Reprinted with permission from ref. [71]. Copyright 2014, Computational Materials Science).

2.3. Simulation of Ti-Al Composite Material

Titanium–aluminum composite panels hold significant applications in the aerospace industry. Due to their lightweight and high-strength characteristics, these panels are ideal for manufacturing structural components for aircraft, rockets, and other aerospace vehicles. They not only reduce the weight of an aircraft and improve fuel efficiency but also offer excellent corrosion resistance, ensuring long-term durability in harsh environments. These benefits are similarly advantageous in the automotive field. The layered ternary compound Ti_2AlN plays a crucial role in reinforcing and toughening TiAl matrix composites due to its unique combination of ceramic and metallic properties [72,73]. Research has also explored the use of graphene as a reinforcing phase. The high defect density in graphene nanosheets induces severe interfacial reactions, leading to the formation of numerous recrystallized nuclei in the matrix, thereby increasing the isometric crystal content [42].

Han et al. [72,74] investigated the Ti_2AlN/TiAl composite using MD simulations, with typical results shown in Figure 4. Atomic models, top and side views of the $Ti_2AlN(0001)$/TiAl(111) coherent interface, and $Ti_2AlN(101(—)3)$/TiAl(111) incoherent interface are displayed in Figure 4a,b. Figure 4c illustrates the interface under uniaxial loading for different strains. The results suggest that micro-voids cannot rapidly propagate along the incoherent interface due to the dual factors of dislocation nucleation and strong bonds. This behavior results in the $Ti_2AlN(101(—)3)$/TiAl(111) incoherent interface system exhibiting ductile fracture behavior.

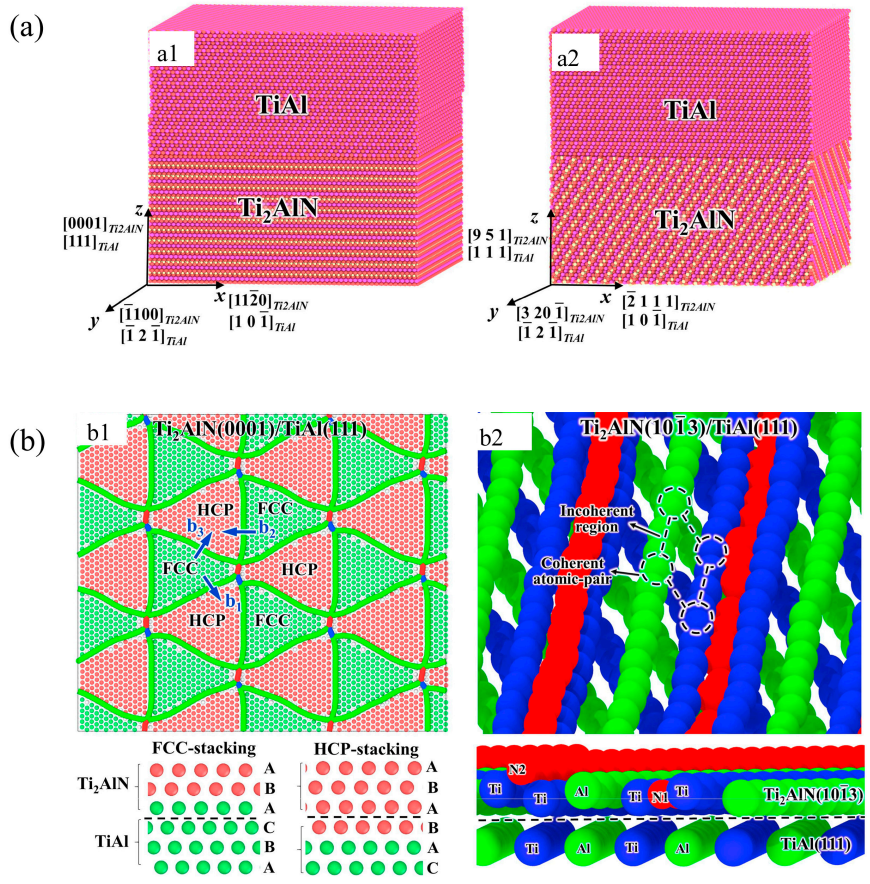

Figure 4. *Cont.*

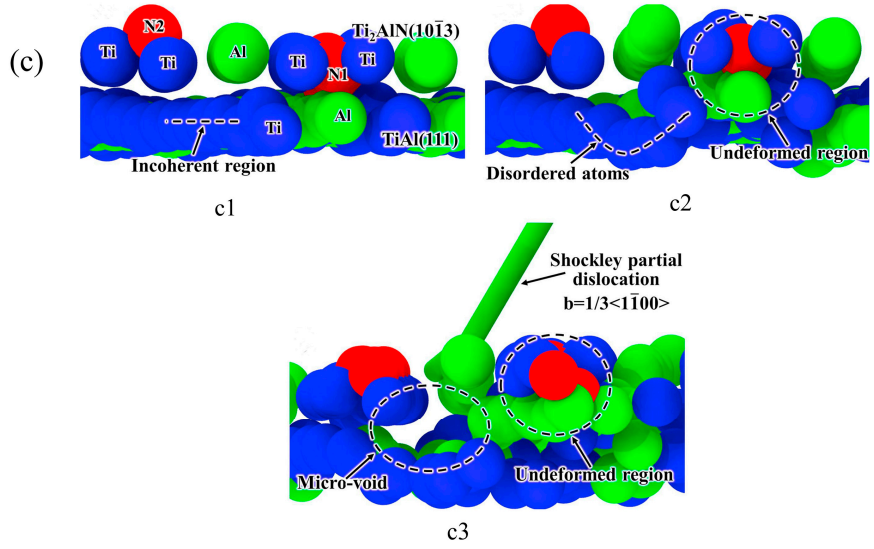

Figure 4. The tensile responses and fracture mechanisms of Ti_2AlN/TiAl composite by MD simulations. (**a**) Atomic models for MD simulation, coherent interface of Ti_2AlN(0001)/TiAl(111) (**a1**), and Ti_2AlN(101(-)3)/TiAl(111) (**a2**). Atoms are color-coded according to their types (Ti in red, Al in pink, and N in yellow). (**b**) Top view (upper portion) and side view (lower portion) of relaxed Ti_2AlN(0001)/TiAl(111) coherent interface (**b1**) and Ti_2AlN(101(-)3)/TiAl(111) incoherent interface atomic structure (**b2**). (**c**) Atomic snapshots under uniaxial loading with different strains. (**c1**) Initial atomic configuration of incoherent interface. (**c2**) Disordered atoms nucleate in the interface. (**c3**) Dislocation nucleates near micro-void. The atoms are color-coded according to their types (Ti in blue, Al in green, and N in red). (Reprinted with permission from ref. [72]. Copyright 2019, Journal of Materials Science).

2.4. Simulation of Ti-Al Alloy Welding

Advancements in lightweight technology have made use of composite structures that combine high-strength and lightweight materials, a viable method for improving the thrust-to-weight ratio of transportation equipment and reducing energy consumption. The Ti/Al composite structure leverages the performance advantages of both titanium and aluminum alloys and holds promising applications in the aerospace, shipbuilding, and automotive industries. Consequently, the welding of Ti and Al has become a critical issue that needs to be addressed. Key research topics in this area include mass transfer principles in laser manufacturing [44,75], the influence of temperature on interfacial diffusion processes [76], and the analysis of welding melting behavior involving titanium–aluminum alloys and titanium–aluminum nanoparticles [77–80].

A notable early study focused on linear friction welding between titanium and aluminum was conducted by Song et al. [81]. This research used MD software to analyze temperature changes, plastic deformation, and atomic diffusion behavior (Figure 5). Different colors in Figure 5a indicate the thermostat layer and Newton layer, while Figure 5b shows temperature changes. Figure 5c,d depict the simulation process and cross-section at different friction times, with the results shown in Figure 5e. The diffusion behavior of aluminum atoms in both directions was nearly identical, whereas self-diffusion of Ti atoms occurred. The applied pressure in the X-direction promoted diffusion. However, due to the influence of pressure, the diffusion of Al into the Ti-based HCP structure was significantly more challenging, as it could not easily overcome the potential barriers caused by atomic diffusion [81].

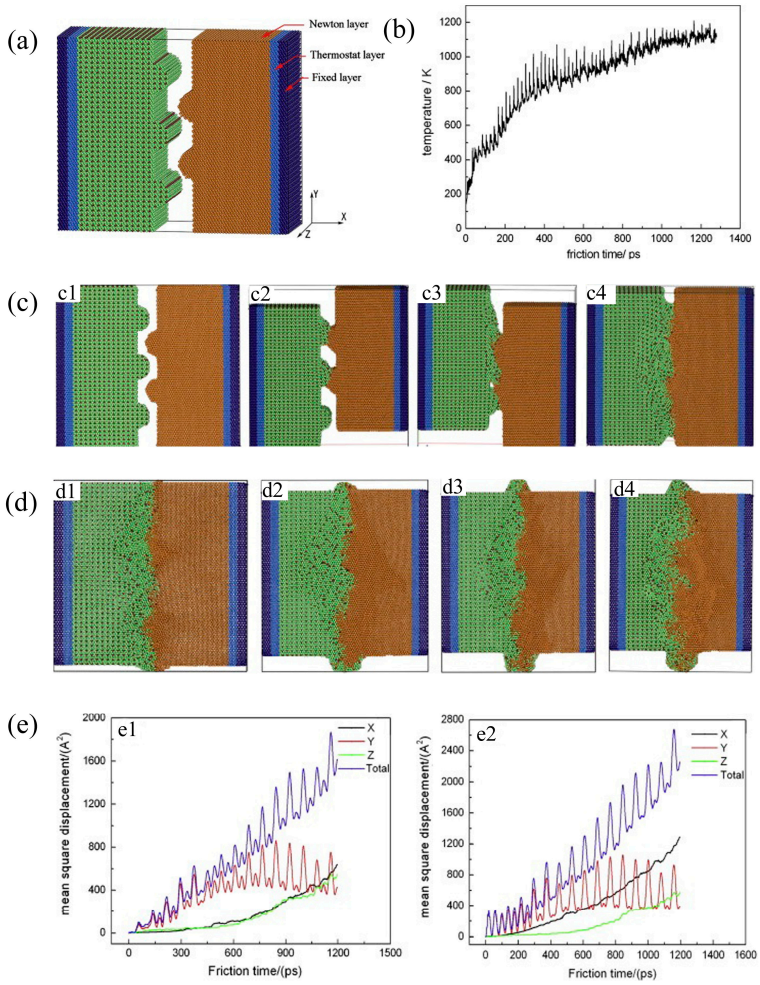

Figure 5. Linear friction welding between dissimilar Ti-based alloys. (**a**) Molecular dynamic simulation model of LFW. (**b**) Temperature profile on the interface of LFW joints. (**c**) Simulation of the LFW process: t = 0 ps (**c1**), t = 5 ps (**c2**), t = 15 ps (**c3**), t = 76 ps (**c4**). (**d**) Configurations of a cross-section with different friction times: t = 200 ps (**d1**), t = 500 ps (**d2**), t = 800 ps (**d3**), and t = 1200 ps (**d4**). (**e**) Mean square displacement results of different atoms: (**e1**) Ti atoms and (**e2**) Al atoms. (Reprinted with permission from ref. [81]. Copyright 2014, Computational Materials Science).

2.5. Simulation of Ti-Al-Based Multi-Layer/Film Materials

Researchers have proposed various mechanisms for strengthening and failure in metal multi-layer composite materials [82]. The strength of these multi-layer/film materials also depends on the initial dislocation density in the constituent layers [83]. For instance, the Al-Ti multi-layer exhibits good thermal stability and minimal mixing at layer thicknesses of 22 nm or more, even at temperatures up to 400 °C [84]. Additionally, annealing aluminum–titanium multi-layer/film materials significantly enhances their hardness, with the hardening effect becoming more pronounced as the layer thickness decreases. Ti-Al-N, used as a ceramic layer, can also resist cracking [85]. Beyond multi-layer materials, there is research on Ti-Al-based films, such as Ti-Al-N [86,87], as well as Ti-coated Al or Al-coated Ti [68,69], and the fabrication of Ti-Al-modified layers to improve the wear resistance of aluminum-based alloys [88].

Sumit Kumar Maurya et al. [89] conducted an atomic analysis of HCP-FCC conversion and redirection in an Al-Ti multi-layer using molecular dynamics software (LAMMPS), as shown in Figure 6. The representative volume element of the Al-Ti multi-layer system is depicted in Figure 6a, while the interface characteristics and relative stresses in the Al-Ti multi-layer are shown in Figure 6b. Figure 6c reveals the redirection mechanism of hexagonal close-packed

Ti [89]. The results indicate that this displacement mechanism involves the formation of an intermediate BCC phase, similar to the one reported by Chen et al. [90].

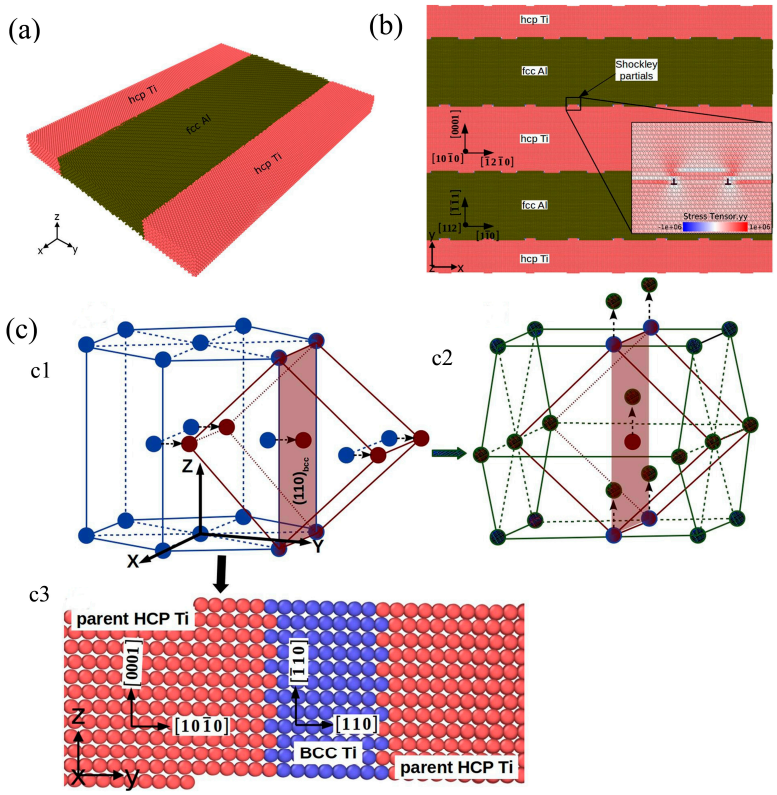

Figure 6. Atomistic analyses of HCP-FCC transformation and reorientation of Ti in Al-Ti multi-layers. (**a**) Representative volume element (RVE) of the Al-Ti multi-layer system used in the present study. The y-dimension of the RVE will change based on the layer thickness. FCC Al atoms are shown in olive color, and HCP Ti atoms are in red. (**b**) Interface characteristics and relative stresses in the Al-Ti multi-layer with configuration A and viewed along the Z-direction. (**c**) Schematic of reorientation mechanism in HCP Ti. (**c1**) shows the unit cell in parent HCP Ti and BCC Ti formed after the first displacement; (**c2**) shows the second displacement and resultant unit cell in reoriented HCP Ti; and (**c3**) is the atomic arrangement of parent HCP Ti (red color) and BCC Ti (blue color). (Reprinted with permission from ref. [89]. Copyright 2021, Computational Materials Science).

2.6. Others

In addition to using MD simulations for two-phase Ti-Al alloys, Ti-Al amorphous alloys, Ti-Al composite materials, Ti-Al welding, and Ti-Al multi-layer/film materials, researchers have also investigated the addition of Ti and Al as reinforcing phases in high-entropy alloys (HEAs). HEAs are alloys formed from five or more metals in equal or approximately equal amounts [91–93]. Due to their desirable properties, HEAs are highly valued in materials science and engineering, characterized by high entropy, lattice distortion, slow diffusion, and the "cocktail" effect [94–96]. MD simulations play a crucial role in revealing and predicting the properties of HEAs at the atomic scale [97–99].

Sun et al. [100] studied CoCrFeNi $(Al_{0.3}Ti_{0.2})_x$ HEAs with varying Ti and Al contents, exploring the effects of content and temperature on mechanical properties. The main research findings are presented in Figure 7. Figure 7a shows the models with different Ti and Al contents established using MD software. The XRD patterns after rolling and the stress–strain tensile characteristics from experiments and MD simulations are depicted in Figure 7b,c. Figure 7d illustrates the dislocation distribution diagrams of the CoCrFeNi$(Al_{0.3}Ti_{0.2})_x$ HEA before fracturing. The analysis indicates that increasing Ti and Al content significantly raises the dislocation density in HEAs, leading to intensified

dislocation intersections. This increases deformation resistance and makes continuous plastic deformation difficult, ultimately enhancing the deformation resistance of the alloy.

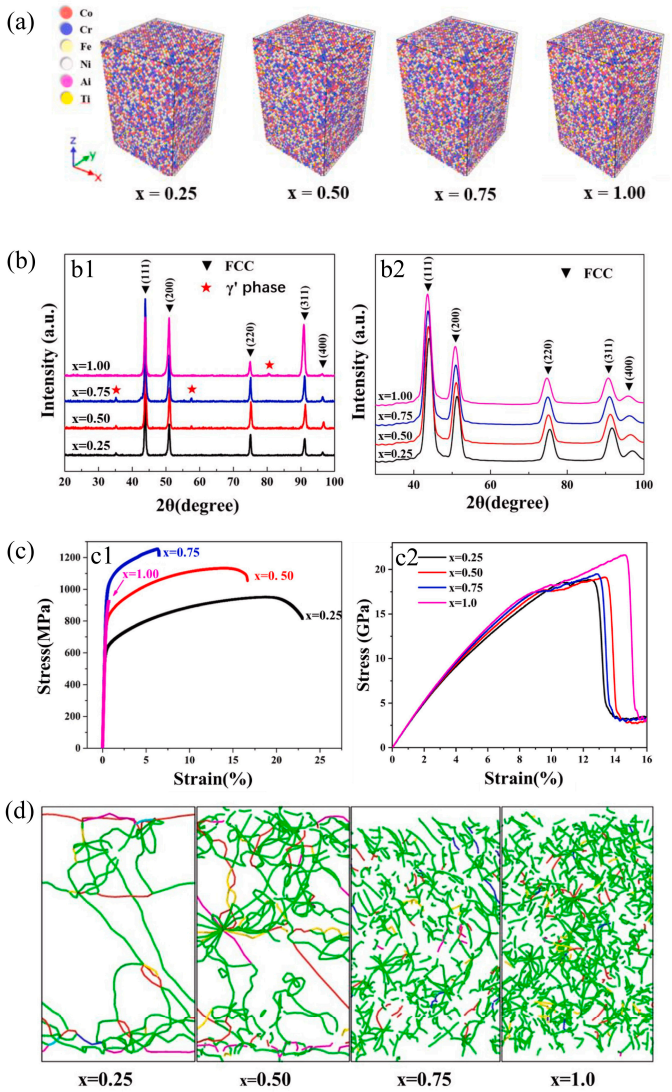

Figure 7. Molecular dynamics simulation of the tensile mechanical properties of CoCrFeNiTiAl high-entropy alloy. (**a**) CoCrFeNi($Al_{0.3}Ti_{0.2}$)$_x$ HEA models with different Ti and Al contents. (**b**) XRD patterns after rolling: (**b1**) experiment and (**b2**) MD simulations. (**c**) Stress–strain tensile characteristics: (**c1**) experimental stress–strain curves at room temperature and (**c2**) MD simulated tensile stress–strain curves. (**d**) Dislocation distribution diagrams before the fracture. (Reprinted with permission from ref. [100]. Copyright 2022, Intermetallics).

A team led by academician Chen Guang [101] from Nanjing University of Science and Technology published a paper in The Innovation Materials, proposing and establishing a dual-phase symbiotic nucleation model. Based on the classical nucleation theory equation, the anisotropy parameter and shape factor of the lamellar interface were introduced to develop the lamellar structure nucleation equation. They derived the critical lamellar nucleation radius, critical lamellar nucleation thickness, and critical nucleation free energy. Theoretical calculations indicated that the free-energy barrier for nucleation of the layered structure during biphasic symbiosis was the smallest and easiest to overcome. Thus, the layered structure nucleates in pairs, rather than the traditional view that A-phase or B-phase nucleates first. They proposed a new biphasic coupled nucleation phenomenon with layered structures, in which two different layered phases nucleate simultaneously from the matrix in pairs, with each pair having independent and heterogeneous nucleation

processes. Through the combination of MD simulation and in situ high-energy synchrotron radiation X-ray diffraction (HEXRD), the experimental observations were further confirmed. This article proposes and establishes a dual-phase symbiotic nucleation model, which has been validated in Ti-Al alloy materials, providing new evidence for the controversy over nucleation mechanisms in the past and enriching the classical nucleation theory, which solves a century-long unresolved problem.

3. Challenges and Further Perspectives

This article summarizes and analyzes MD simulations of various Ti-Al-based alloys, including Ti-Al alloys, Ti-Al amorphous alloys, Ti-Al composite materials, Ti-Al welding, and Ti-Al multi-layer materials. MD simulations offer valuable insights into the structure and properties of different materials under various conditions. This review provides an overview of the application of MD simulations in studying different Ti-Al alloys. To achieve the best results, it is crucial to fully consider the characteristics of the target material and select an appropriate starting configuration. Additionally, the size of the force field file and the system significantly impact the accuracy of the simulations. It is also essential to consider system energy minimization and relaxation phenomena to obtain more accurate data.

Figure 8 shows an overview of the research on Ti-Al-based alloys. Figure 8a expresses a keyword clustering view of the published literature on Ti-Al from 2009 to the present. It can be seen that many scholars have conducted generous and extensive research in these years. Figure 8b is the histograms of publication numbers and citation frequency of relevant articles retrieved with the keywords "Ti-Al" in the Web of Science database. The graph indicates that research in this area has grown rapidly in recent years, with the citation frequency reaching 12,349 times in 2023. The introduction of MD simulation methods has further utilized the development of research on Ti-Al since it is a very powerful tool. However, there is still considerable room for development.

1. Comprehensive database of Ti-Al alloys: Over the past few decades, extensive research on the preparation processes and properties of Ti-Al alloys has generated a wealth of data. However, due to compositional variations among different Ti-Al alloys and the lack of high-quality data, there is a need for a comprehensive Ti-Al alloy database. This database should include detailed information on alloy compositions, preparation methods, and performance characteristics. Such a resource would significantly accelerate the research and development efforts aimed at optimizing the performance of Ti-Al alloys. Here is a summary for reference only. Firstly, it is the collecting and processing of data in the Ti-Al alloy material database. The author can access authoritative information on Ti-Al alloys both domestically and internationally through material manuals related to Ti-Al alloys and standards, as well as renowned academic journals and conference proceedings. Secondly, the database design is an extremely important step that directly affects the writing of program codes, the stability, and the speed of system operations simultaneously. It is the key to the success or failure of developing a data information management system. Thirdly, the complex system is decomposed into relatively independent and functionally single modules. Each module can be designed, written, and debugged separately. Finally, each module can be integrated organically, according to their subordinate relationships, and a database system can be built that meets the functional requirements, owns a clear hierarchy, and has a reasonable structure. This database enables intelligent query methods from multiple perspectives and levels to accurately obtain data information, freeing researchers from the tedious task of flipping through manuals and greatly improving efficiency.

2. Cross-scale computational techniques for Ti-Al alloys: Integrating computational models with experimental research can provide a detailed understanding of the microstructure evolution of Ti-Al alloys and their impact on macroscopic properties. This method can tightly integrate MD simulation with density functional theory (DFT) and the finite element method (FEM) and enhance the understanding of the relationship between microstructure and the properties of Ti-Al alloys. The ab initio MD simulation developed in recent years

is based on density functional theory [102]. Mohamed et al. focus on understanding the interfacial traction–separation in Ti6Al4V/TiC using MD simulations, and FEM is carried out to determine the bulk properties and the debonding behavior in Ti6Al4V/TiC under compression [103].

3. Development of improved potential energy functions: Creating potential energy functions that more accurately describe atomic interactions while maintaining manageable computational complexity will yield more realistic simulation results. Such as when Pei et al. examined four interatomic potentials (two EAM and two MEAM) developed for the Ti-Al material system, and one MEAM potential reproduced some of the properties. Then it was found that further optimization of the parameters in the MEAM formalism may lead to better interatomic potentials for the Ti-Al system [104].

4. Advancements in computational power: Although improvements in computational power have increased the modeling size and simulation time, there remains a significant gap between the actual workpiece sizes and the duration required for experimental processes. Bridging this gap will be essential for achieving more practical and applicable simulation results. In recent years, with the development of high-performance computing technology and the application of parallel computing and cloud computing, molecular dynamics simulations can achieve larger and more complex systems, as well as longer time and scale dynamic processes. For example, combining with machine learning [105].

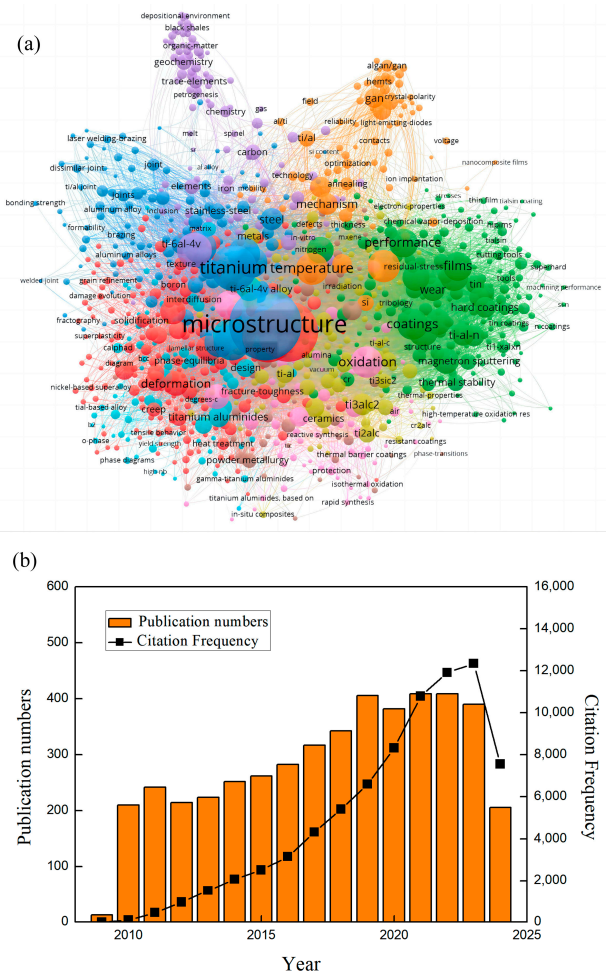

Figure 8. An overview of the research on Ti-Al-based alloys. (**a**) Keyword network visualization in the Ti-Al literature from the Web of Science database. (**b**) A histogram of the publication number and citation frequency of relevant articles retrieved with the keywords "Ti-Al" in the Web of Science database.

Author Contributions: Writing—original draft preparation, N.L.; conceptualization, N.L. and Z.H.; methodology, N.L. and Z.H.; writing—review and editing, L.X. and L.W. (Lifei Wang); investigation, N.L. and L.W. (Leyu Wei); formal analysis, N.L. and M.T.; data curation, L.X. and L.W. (Lifei Wang); resources, L.W. (Leyu Wei) and M.T.; supervision L.X. and L.W. (Lifei Wang). All authors have read and agreed to the published version of the manuscript.

Funding: This research was funded by the Natural Science Foundation of Shanxi province (No. 20210302123163), the Central Government Guided Local Science and Technology Development projects (No. YDZJSX2021A010), the China Postdoctoral Science Foundation (No. 2022M710541), and the High-Level Introduction of Talent Research Start-Up and Electric Power (No. 4001/40680).

Data Availability Statement: No new data were created or analyzed in this study. Data sharing is not applicable to this article.

Acknowledgments: I would like to express my deepest gratitude to Shuai Li from the School of Mechanical Engineering at North China University of Water Resources and Electric Power for providing me with valuable methodological guidance on the writing.

Conflicts of Interest: The authors declare no conflicts of interest.

References

1. Pradeep, G.V.K.; Duraiselvam, M.; Sivaprasad, K. Tribological behavior of laser surface melted γ-TiAl fabricated by electron beam additive manufacturing. *J. Mater. Eng. Perform.* **2022**, *31*, 1009–1020. [CrossRef]
2. Tan, Y.; Wang, Y.; You, X.; Liu, H.; Li, P. Effect of solution heat treatment on the microstructure and hardness of theTi-48Al-2Cr-2Nb alloy prepared by electron beam smelting. *J. Mater. Eng. Perform.* **2022**, *31*, 1387–1396. [CrossRef]
3. Mohammadnejad, A.; Bahrami, A.; Tafaghodi Khajavi, L. Microstructure and mechanical properties of spark plasma sintered nanocrystalline TiAl-x B composites (0.0 < x < 1.5 at.%) containing carbon nanotubes. *J. Mater. Eng. Perform.* **2021**, *30*, 4380–4392.
4. Zha, M.; Wang, H.Y.; Li, S.T.; Li, S.L.; Guan, Q.L.; Jiang, Q.C. Influence of Al addition on the products of self-propagating high-temperature synthesis of Al-Ti-Si system. *Mater. Chem. Phys.* **2009**, *114*, 709–715. [CrossRef]
5. Liu, Y.; Hu, R.; Kou, H.C.; Wang, J.; Zhang, T.B.; Li, J.S.; Zhang, J. Solidification characteristics of high Nb-containing γ-TiAl-based alloys with different aluminum contents. *Rare Met.* **2015**, *34*, 381–386. [CrossRef]
6. Bizot, Q.; Politano, O.; Nepapushev, A.A.; Vadchenko, S.G.; Rogachev, A.S.; Baras, F. Reactivity of the Ti-Al system: Experimental study and molecular dynamics simulations. *J. Appl. Phys.* **2020**, *127*, 145304. [CrossRef]
7. Tian, Y.; Shen, J.; Hu, S.; Gou, J.; Cui, Y. Effects of cold metal transfer mode on the reaction layer of wire and arc additive-manufactured Ti-6Al-4V/Al-6.25 Cu dissimilar alloys. *J. Mater. Sci. Technol.* **2021**, *74*, 35–45. [CrossRef]
8. Rittinghaus, S.K.; Wilms, M.B. Oxide dispersion strengthening of γ-TiAl by laser additive manufacturing. *J. Alloys Compd.* **2019**, *804*, 457–460. [CrossRef]
9. Yang, J.; Xiao, S.; Zhang, Q.K.; Xu, C.; Li, W.D.; Zheng, B.Z.; Hu, F.Q.; Yin, J.; Song, Z.L. In-situ synthesis of Ti-Al intermetallic compounds coating on Ti alloy by magnetron sputtering deposition followed by vacuum annealing. *Vacuum* **2020**, *172*, 109060. [CrossRef]
10. Chen, G.; Peng, Y.; Zheng, G.; Qi, Z.; Wang, M.; Yu, H.; Dong, C.; Liu, C.T. Polysynthetic twinned TiAl single crystals for high-temperature applications. *Nat. Mater.* **2016**, *15*, 876–881. [CrossRef]
11. Shagiev, M.R.; Galeyev, R.M.; Valiakhmetov, O.R.; Safiullin, R.V. Improved mechanical properties of Ti_2AlNb-based intermetallic alloys and composites. *Adv. Mater. Res.* **2009**, *59*, 105–108. [CrossRef]
12. Wang, D.P.; Qi, Z.X.; Zhang, H.T.; Chen, G.; Lu, Y.; Sun, B.A.; Liu, C.T. Microscale mechanical properties of ultra-high-strength polysynthetic TiAl-Ti_3Al single crystals. *Mater. Sci. Eng. A* **2018**, *732*, 14–20. [CrossRef]
13. Djanarthany, S.; Viala, J.-C.; Bouix, J. An overview of monolithic titanium aluminides based on Ti_3Al and TiAl. *Mater. Chem. Phys.* **2001**, *72*, 301–319. [CrossRef]
14. Cao, S.Z.; Xiao, S.L.; Chen, Y.Y.; Xu, L.J.; Wang, X.P.; Han, J.C.; Jia, Y. Phase transformations of the $L1_2$-Ti_3Al phase in γ-TiAl alloy. *Mater. Design.* **2017**, *121*, 61–68. [CrossRef]
15. Avdeeva, V.; Bazhina, A.; Antipov, M.; Stolin, A.; Bazhin, P. Relationship between structure and properties of intermetallic materials based on γ-TiAl hardened in situ with Ti_3Al. *Metals* **2023**, *13*, 1002. [CrossRef]
16. Wimler, D.; Lindemann, J.; Kremmer, T.; Clemens, H.; Mayer, S. Microstructure and mechanical properties of novel TiAl alloys tailored via phase and precipitate morphology. *Intermetallics* **2021**, *138*, 107316. [CrossRef]
17. Zhang, H.; Yan, N.; Liang, H.; Liu, Y. Phase transformation and microstructure control of Ti_2AlNb-based alloys: A review. *J. Mater. Sci. Technol.* **2021**, *80*, 203–216. [CrossRef]
18. Hussain, A.; Mehmood, S.; Rasool, N.; Li, N.; Dharmawardhana, C.C. Electronic structure, mechanical and optical properties of $TiAl_3$ ($L1_2$ & $D0_{22}$) via first-principles calculations. *Chin. J. Phys.* **2016**, *54*, 319–328.
19. Xie, Y.Q.; Liu, X.B.; Peng, K.; Peng, H.J. Atomic states, potential energies, volumes, stability, and brittleness of ordered FCC $TiAl_3$-type alloys. *Phys. B* **2004**, *353*, 15–33. [CrossRef]

20. Xie, Z.C.; Gao, T.H.; Guo, X.T.; Xie, Q. Molecular dynamics simulation of nanocrystal formation and deformation behavior of Ti_3Al alloy. *Comp. Mater. Sci.* **2015**, *98*, 245–251. [CrossRef]
21. Xu, S.; Wan, Q.; Sha, Z.; Liu, Z. Molecular dynamics simulations of nano-indentation and wear of the γTi-Al alloy. *Comp. Mater. Sci.* **2015**, *110*, 247–253. [CrossRef]
22. Poletaev, G.M. Self-diffusion in liquid and solid alloys of the Ti-Al system: Molecular dynamics simulation. *J. Exp. Theor. Phys.* **2021**, *133*, 455–460. [CrossRef]
23. Becquart, C.S.; Decker, K.M.; Domain, C.; Ruste, J.; Souffez, Y.; Turbatte, J.C.; Van Duysen, J.C. Massively parallel molecular dynamics simulations with EAM potentials. *Radiat. Eff. Defects Solids* **1997**, *142*, 9–21. [CrossRef]
24. Hollingsworth, S.A.; Dror, R.O. Molecular dynamics simulation for all. *Neuron* **2018**, *99*, 1129–1143. [CrossRef] [PubMed]
25. Tuckerman, M.E.; Martyna, G.J. Understanding modern molecular dynamics: Techniques and applications. *J. Phys. Chem. B* **2000**, *104*, 159–178. [CrossRef]
26. Karplus, M.; McCammon, J.A. Molecular dynamics simulations of biomolecules. *Nat. Struct. Biol.* **2002**, *9*, 646–652. [CrossRef]
27. Zepeda-Ruiz, L.A.; Stukowski, A.; Oppelstrup, T.; Bulatov, V.V. Probing the limits of metal plasticity with molecular dynamics simulations. *Nature* **2017**, *550*, 492–495. [CrossRef]
28. Sankar, N.; Mathew, N.; Sobhan, C.B. Molecular dynamics modeling of thermal conductivity enhancement in metal nanoparticle suspensions. *Int. Commun. Heat Mass Transf.* **2008**, *35*, 867–872. [CrossRef]
29. Wang, M.; Jiang, S.; Sun, D.; Zhang, Y.; Yan, B. Molecular dynamics simulation of mechanical behavior and phase transformation of nanocrystalline NiTi shape memory alloy with gradient structure. *Comp. Mater. Sci.* **2022**, *204*, 111186. [CrossRef]
30. Singh, A.; Kumar, D. Effect of temperature on elastic properties of CNT-polyethylene nanocomposite and its interface using MD simulations. *J. Mol. Model.* **2018**, *24*, 178. [CrossRef]
31. Sri Harish, M.; Patra, P.K. Temperature and its control in molecular dynamics simulations. *Mol. Simulat.* **2021**, *47*, 701–729. [CrossRef]
32. Lu, X.; Ran, H.; Cheng, Q.; Guo, F.; Huang, C. Underlying mechanisms of enhanced plasticity in Ti/Al laminates at elevated temperatures: A molecular dynamics study. *J. Mater. Res. Technol.* **2024**, *28*, 31–42. [CrossRef]
33. Pogorelko, V.V.; Mayer, A.E. Dynamic tensile fracture of iron: Molecular dynamics simulations and micromechanical model based on dislocation plasticity. *Int. J. Plast.* **2023**, *167*, 103678. [CrossRef]
34. Shuang, F.; Aifantis, K.E. Modelling dislocation-graphene interactions in a BCC Fe matrix by molecular dynamics simulations and gradient plasticity theory. *Appl. Surf. Sci.* **2021**, *535*, 147602. [CrossRef]
35. Zhou, J.; Shen, J.; Yue, W.; Liu, Y.; Chen, Z. Molecular dynamics simulation of reinforcement mechanism of graphene/aluminum composites and microstructure evolution. *J. Mater. Res. Technol.* **2023**, *23*, 2147–2159. [CrossRef]
36. Medyanik, S.N.; Shao, S. Strengthening effects of coherent interfaces in nanoscale metallic bilayers. *Comp. Mater. Sci.* **2009**, *45*, 1129–1133. [CrossRef]
37. Shimono, M.; Onodera, H. Molecular dynamics study on formation and crystallization of Ti–Al amorphous alloys. *Mater. Sci. Eng. A* **2001**, *304*, 515–519. [CrossRef]
38. Song, H.; Gao, T.; Gao, Y.; Liu, Y.; Xie, Q.; Chen, Q.; Xiao, Q.Q.; Liang, Y.C.; Wang, B. Hall-Petch relationship in Ti_3Al nano-polycrystalline alloys by molecular dynamics simulation. *J. Mater. Sci.* **2022**, *57*, 20589–20600. [CrossRef]
39. Pei, Q.X.; Lu, C.; Fu, M.W. The rapid solidification of Ti_3Al: A molecular dynamics study. *J. Phys: Condens. Matter* **2004**, *16*, 4203. [CrossRef]
40. Han, X.J.; Chen, M.; Guo, Z.Y. A molecular dynamics study for the thermophysical properties of liquid Ti–Al alloys. *Int. J. Thermophys.* **2005**, *26*, 869–880. [CrossRef]
41. Polyakova, P.V.; Shcherbinin, S.A.; Baimova, J.A. Molecular dynamics investigation of atomic mixing and mechanical properties of Al/Ti interface. *Lett. Mater.* **2021**, *11*, 561–565. [CrossRef]
42. Gao, T.; He, H.; Liu, Y.; Bian, Z.; Chen, Q.; Xie, Q.; Liang, Y.; Xiao, Q. Molecular dynamics simulation of dislocation network formation and tensile properties of graphene/TiAl-layered composites. *Surf. Interfaces* **2023**, *39*, 102983. [CrossRef]
43. Wu, X.M.; Shi, C.G.; Wang, H.T.; Luo, X.C.; Sun, Z.R. Atomic motion behavior calculation and bonding mechanism analysis of explosive welding of high-strength and high-hardness titanium alloy Ti6Al4V/aluminum alloy 7075. *Mater. Res. Express* **2023**, *10*, 106518.
44. Cui, Z.; Zhou, X.; Meng, Q. Atomic-scale mechanism investigation of mass transfer in laser fabrication process of Ti-Al alloy via molecular dynamics simulation. *Metals* **2020**, *10*, 1660. [CrossRef]
45. Kiselev, S.P.; Zhirov, E.V. Molecular-dynamics simulation of the synthesis of intermetallic Ti–Al. *Intermetallics* **2014**, *49*, 106–114. [CrossRef]
46. Poletaev, G.M.; Bebikhov, Y.V.; Semenov, A.S.; Starostenkov, M.D. Self-diffusion in melts of Ni-Al and Ti-Al systems: Molecular dynamics study. *Lett. Mater.* **2021**, *11*, 438–441. [CrossRef]
47. Guo, F.; Holec, D.; Wang, J.; Li, S.; Du, Y. Impact of V, Hf and Si on oxidation processes in Ti-Al-N: Insights from ab initio molecular dynamics. *Surf. Coat. Technol.* **2020**, *381*, 125125. [CrossRef]
48. Xia, J.H.; Liu, C.S.; Cheng, Z.F.; Shi, D.P. Molecular dynamics simulations on local structure and diffusion in liquid Ti_xAl_{1-x} alloys. *Phys. B* **2011**, *406*, 3938–3941. [CrossRef]
49. Zhang, B.; Zhang, X.; Li, C.; Zhou, K. Molecular dynamics simulation on phase transformation of Ti-Al alloy with low Al content. *Rare Metal Mater. Eng.* **2012**, *41*, 1010–1015. [CrossRef]

50. Venkataraman, A.; Shade, P.A.; Adebisi, R.; Sathish, S.; Pilchak, A.L.; Viswanathan, G.B.; Brandes, M.C.; Mills, M.J.; Sangid, M.D. Study of structure and deformation pathways in Ti-7Al using atomistic simulations, experiments, and characterization. *Metall. Mater. Trans. A* **2017**, *48*, 2222–2236. [CrossRef]
51. Arifin, R.; Setiawan, D.R.P.; Triawan, D.; Putra, A.F.S.; Munaji; Winardi, Y.; Putra, W.T.; Darminto. Structural transformation of Ti-based alloys during tensile and compressive loading: An insight from molecular dynamics simulations. *MRS Commun.* **2023**, *13*, 225–232. [CrossRef]
52. Li, T.; Tian, C.; Moridi, A.; Yeo, J. Elucidating interfacial dynamics of Ti-Al systems using molecular dynamics simulation and markov state, odeling. *ACS Appl. Mater. Interfaces* **2023**, *15*, 50489–50498. [CrossRef]
53. Liu, J.; Zhang, L. Investigation on the diffusion behaviors and mechanical properties of the Ti/Al interface using molecular dynamics simulation. *J. Mater. Eng. Perform.* **2024**, *33*, 2920–2939. [CrossRef]
54. Hui, C.; Zhiyuan, R.; Wenke, C.; Ruicheng, F.; Changfeng, Y. Deformation mechanisms in nanotwinned γ-TiAl by molecular dynamics simulation. *Mol. Simulat.* **2018**, *44*, 1489–1500. [CrossRef]
55. Liu, J.; Zhang, L. Molecular dynamics simulation of the tensile deformation behavior of the γ (TiAl)/α_2(Ti_3Al) interface at different temperatures. *J. Mater. Eng. Perform.* **2022**, *31*, 918–932. [CrossRef]
56. Xu, D.S.; Wang, H.; Yang, R.; Veyssiere, P. Molecular dynamics investigation of deformation twinning in γ-TiAl sheared along the pseudo-twinning direction. *Acta Mater.* **2008**, *56*, 1065–1074. [CrossRef]
57. Kim, J.H.; Lee, S.H. Molecular dynamics simulation studies of benzene, toluene, and p-xylene in NpT ensemble: Thermodynamic, structural, and dynamic properties. *Bull.-Korean Chem. Soc.* **2002**, *23*, 447–458.
58. Wu, H.N.; Xu, D.S.; Wang, H.; Yang, R. Molecular dynamics simulation of tensile deformation and fracture of γ-TiAl with and without surface defects. *J. Mater. Sci. Technol.* **2016**, *32*, 1033–1042. [CrossRef]
59. Liu, Y.; Gao, T.; Gao, Y.; Li, L.; Tan, M.; Xie, Q.; Chen, Q.; Tian, Z.; Liang, Y.; Wang, B. Evolution of defects and deformation mechanisms in different tensile directions of solidified lamellar Ti–Al alloy. *Chin. Phys. B* **2022**, *31*, 046105. [CrossRef]
60. Zhang, H.; Wei, B.; Ou, X.; Ni, S.; Yan, H.; Song, M. Atomic-level study of {10 1} deformation twinning in pure Ti and Ti-5 at.% Al alloy. *Int. J. Plast.* **2022**, *153*, 103273. [CrossRef]
61. Xu, T.T.; Li, J.Y.; Xiao, R.L.; Qin, J.Y.; Ruan, Y.; Li, H. The mixing enthalpy and liquid structural properties of Ti–Al alloys by ab inito molecular dynamics simulation. *J. Phase Equilib. Diff.* **2022**, *43*, 585–593. [CrossRef]
62. Sun, R.; Mi, G.; Huang, X.; Sui, N. Molecular dynamic simulations of Ti-6Al and Fe-12Cr alloys for their heat transfer and oxygen transport behaviors. *Mod. Phys. Lett. B* **2024**, *38*, 2350263. [CrossRef]
63. Feng, R.; Song, W.; Li, H.; Qi, Y.; Qiao, H.; Li, L. Effects of annealing on the residual stress in γ-TiAl alloy by molecular dynamics simulation. *Materials* **2018**, *11*, 1025. [CrossRef] [PubMed]
64. Ganesan, H.; Scheider, I.; Cyron, C.J. Quantifying the high-temperature separation behavior of Lamellar interfaces in γ-titanium aluminide under tensile loading by molecular dynamics. *Front. Mater.* **2021**, *7*, 602567. [CrossRef]
65. Voskoboinikov, R.E. Molecular dynamics simulations of radiation damage in $D0_{19}$ Ti_3Al intermetallic compound. *Nucl. Instrum. Meth. B* **2013**, *307*, 25–28. [CrossRef]
66. Shimono, M.; Onodera, H. Molecular dynamics study on liquid-to-amorphous transition in Ti–Al alloys. *Mater. Trans. JIM* **1998**, *39*, 147–153. [CrossRef]
67. Chu, J.J.; Steeves, C.A. Thermal expansion and recrystallization of amorphous Al and Ti: A molecular dynamics study. *J. Non-Cryst. Solids* **2011**, *357*, 3765–3773. [CrossRef]
68. Levchenko, E.V.; Evteev, A.V.; Löwisch, G.G.; Belova, I.V.; Murch, G.E. Molecular dynamics simulation of alloying in a Ti-coated Al nanoparticle. *Intermetallics* **2012**, *22*, 193–202. [CrossRef]
69. Levchenko, E.V.; Evteev, A.V.; Lorscheider, T.; Belova, I.V.; Murch, G.E. Molecular dynamics simulation of alloying in an Al-coated Ti nanoparticle. *Comp. Mater. Sci.* **2013**, *79*, 316–325. [CrossRef]
70. Tahiri, M.; Hassani, A.; Sbiaai, K.; Hasnaoui, A. Investigating local atomic structural order in $TiAl_3$ metallic glass using molecular dynamic simulation. *Comput. Condens. Matter* **2018**, *14*, 74–83. [CrossRef]
71. Xie, Z.C.; Gao, T.H.; Guo, X.T.; Qin, X.M.; Xie, Q. Glass formation and icosahedral medium-range order in liquid Ti-Al alloys. *Comp. Mater. Sci.* **2014**, *95*, 502–508. [CrossRef]
72. Han, X.; Liu, P.; Sun, D.; Wang, Q. Quantifying the role of interface atomic structure in the compressive response of Ti_2AlN/TiAl composite using MD simulations. *J. Mater. Sci.* **2019**, *54*, 5536–5550. [CrossRef]
73. Duong, T.C.; Singh, N.; Arróyave, R. First-principles calculations of finite-temperature elastic properties of Ti_2AlX (X=C or N). *Comp. Mater. Sci.* **2013**, *79*, 296–302. [CrossRef]
74. Han, X.; Liu, P.; Sun, D.; Wang, Q. Molecular dynamics simulations of the tensile responses and fracture mechanisms of Ti_2AlN/TiAl composite. *Theor. Appl. Fract. Mech.* **2019**, *101*, 217–223. [CrossRef]
75. Zhang, Y.F.; Li, Q.; Gong, M.; Xue, S.; Ding, J.; Li, J.; Cho, J.; Niu, T.; Su, R.; Richter, N.A. Deformation behavior and phase transformation of nanotwinned Al/Ti multilayers. *Appl. Surf. Sci.* **2020**, *527*, 146776. [CrossRef]
76. Li, P.; Wang, L.; Yan, S.; Meng, M.; Xue, K. Temperature effect on the diffusion welding process and mechanism of B2-O interface in the Ti_2AlNb-based alloy: A molecular dynamics simulation. *Vacuum* **2020**, *173*, 109118. [CrossRef]
77. Ou, P.; Cao, Z.; Rong, J.; Yu, X. Molecular dynamics study on the welding behavior in dissimilar TC4-TA17 titanium alloys. *Materials* **2022**, *15*, 5606. [CrossRef]

78. Zhang, H.; Su, Y.C.; Han, Y.; Jiang, S. Molecular dynamics study of melting behavior of planar stacked Ti–Al core–shell nanoparticles. *J. Compos. Sci.* **2022**, *6*, 126. [CrossRef]
79. Wang, L.; Chen, Y.; Xia, X.; Zhang, Z.; Wang, T.; Zhang, H. A molecular dynamics simulation-based laser melting behavior analysis for Ti–Al binary alloy. *Int. J. Mod. Phys. B* **2023**, *37*, 2350196. [CrossRef]
80. Moon, S.; Paek, J.H.; Jang, Y.H.; Kang, K. Mixing behavior of Ti–Al interface during the ultrasonic welding process and its welding strength: Molecular dynamics study. *Heliyon* **2024**, *10*, e25116. [CrossRef]
81. Song, C.; Lin, T.; He, P.; Jiao, Z.; Tao, J.; Ji, Y. Molecular dynamics simulation of linear friction welding between dissimilar Ti-based alloys. *Comp. Mater. Sci.* **2014**, *83*, 35–38. [CrossRef]
82. Zhou, X.; Chen, C. Strengthening and toughening mechanisms of amorphous/amorphous nanolaminates. *Int. J. Plast.* **2016**, *80*, 75–85. [CrossRef]
83. Salehinia, I.; Wang, J.; Bahr, D.F.; Zbib, H.M. Molecular dynamics simulations of plastic deformation in Nb/NbC multilayers. *Int. J. Plast.* **2014**, *59*, 119–132. [CrossRef]
84. Zhang, Y.F.; Su, R.; Niu, T.J.; Richter, N.A.; Xue, S.; Li, Q.; Ding, J.; Yang, B.; Wang, H.; Zhang, X. Thermal stability and deformability of annealed nanotwinned Al/Ti multilayers. *Scr. Mater.* **2020**, *186*, 219–224. [CrossRef]
85. Wang, C.; Shi, K.; Gross, C.; Pureza, J.M.; de Mesquita Lacerda, M.; Chung, Y.W. Toughness enhancement of nanostructured hard coatings: Design strategies and toughness measurement techniques. *Surf. Coat. Technol.* **2014**, *257*, 206–212. [CrossRef]
86. Shugurov, A.R.; Panin, A.V.; Dmitriev, A.I.; Nikonov, A.Y. Multiscale fracture of Ti-Al-N coatings under uniaxial tension. *Phys. Mesomech.* **2021**, *24*, 185–195. [CrossRef]
87. Wang, S.; Zhang, J.; Kong, Y.; Chen, L.; Du, Y. Influence of oxygen addition on the oxidation resistance of TiAlN. *Scr. Mater.* **2023**, *224*, 115148. [CrossRef]
88. Tang, G.; Ou, Z.; Liu, F.; Li, T.; Su, F.; Zheng, J.; Liang, Z. Enhancing wear resistance of aluminum alloy by fabricating a Ti-Al modified layer via surface mechanical attrition treatment. *Tribol. Int.* **2024**, *193*, 109462. [CrossRef]
89. Maurya, S.K.; Nie, J.F.; Alankar, A. Atomistic analyses of HCP-FCC transformation and reorientation of Ti in Al-Ti multilayers. *Comp. Mater. Sci.* **2021**, *192*, 110329. [CrossRef]
90. Chen, P.; Wang, F.; Li, B. Transitory phase transformations during {102} twinning in titanium. *Acta Mater.* **2019**, *171*, 65–78. [CrossRef]
91. George, E.P.; Raabe, D.; Ritchie, R.O. High-entropy alloys. *Nat. Rev. Mater.* **2019**, *4*, 515–534. [CrossRef]
92. Zhang, Y.; Zuo, T.T.; Tang, Z.; Gao, M.C.; Dahmen, K.A.; Liaw, P.K.; Lu, Z.P. Microstructures and properties of high-entropy alloys. *Prog. Mater. Sci.* **2014**, *61*, 1–93. [CrossRef]
93. Li, W.; Xie, D.; Li, D.; Zhang, Y.; Gao, Y.; Liaw, P.K. Mechanical behavior of high-entropy alloys. *Prog. Mater. Sci.* **2021**, *118*, 100777. [CrossRef]
94. Miracle, D.B.; Senkov, O.N. A critical review of high entropy alloys and related concepts. *Acta Mater.* **2017**, *122*, 448–511. [CrossRef]
95. Yeh, J.W.; Chen, Y.L.; Lin, S.J.; Chen, S.K. High-entropy alloys—A new era of exploitation. *Mater. Sci. Forum* **2007**, *560*, 1–9. [CrossRef]
96. Zhang, W.; Liaw, P.K.; Zhang, Y. Science and technology in high-entropy alloys. *Sci. China Mater.* **2018**, *61*, 2–22. [CrossRef]
97. Li, J.; Fang, Q.; Liu, B.; Liu, Y.; Liu, Y. Mechanical behaviors of AlCrFeCuNi high-entropy alloys under uniaxial tension via molecular dynamics simulation. *RSC Adv.* **2016**, *6*, 76409–76419. [CrossRef]
98. Chen, K.T.; Wei, T.J.; Li, G.C.; Chen, M.Y.; Chen, Y.S.; Chang, S.W.; Yen, H.W.; Chen, C.S. Mechanical properties and deformation mechanisms in CoCrFeMnNi high entropy alloys: A molecular dynamics study. *Mater. Chem. Phys.* **2021**, *271*, 124912. [CrossRef]
99. Jiang, J.; Chen, P.; Qiu, J.; Sun, W.; Saikov, I.; Shcherbakov, V.; Alymov, M. Microstructural evolution and mechanical properties of Al_xCoCrFeNi high-entropy alloys under uniaxial tension: A molecular dynamics simulations study. *Mater. Today Commun.* **2021**, *28*, 102525. [CrossRef]
100. Sun, Z.H.; Zhang, J.; Xin, G.X.; Xie, L.; Yang, L.C.; Peng, Q. Tensile mechanical properties of CoCrFeNiTiAl high entropy alloy via molecular dynamics simulations. *Intermetallics* **2022**, *142*, 107444. [CrossRef]
101. Zheng, G.; Chen, Y.; Xiang, H.; Zhang, J.; Tu, K.N.; Feng, C.; Li, P.; Song, L.; Sha, G.; Qi, Z. Coupled nucleation of dual-phase lamellar structure. *Innov. Mater.* **2023**, *1*, 100043. [CrossRef]
102. Li, Z.; Feng, Y.; Wen, Y.; Peng, X.; Cai, Z.; Peng, C.; Wang, R. Ab initio molecular dynamics study on the local structures and solid/liquid interface in liquid Al-Ti and Al-B-Ti alloys. *Mater. Today Commun.* **2024**, *39*, 109290. [CrossRef]
103. Elkhateeb, M.G.; Shin, Y.C. Molecular dynamics-based cohesive zone representation of Ti6Al4V/TiC composite interface. *Mater. Des.* **2018**, *155*, 161–169. [CrossRef]
104. Pei, Q.X.; Jhon, M.H.; Quek, S.S.; Wu, Z. A systematic study of interatomic potentials for mechanical behaviours of Ti-Al alloys. *Comp. Mater. Sci.* **2021**, *188*, 110239. [CrossRef]
105. Zhai, B.; Wang, H.P. Accurate interatomic potential for the nucleation in liquid Ti-Al binary alloy developed by deep neural network learning method. *Comp. Mater. Sci.* **2023**, *216*, 111843. [CrossRef]